Thin Solid Films 545 (2013) 171–175

Contents lists available at ScienceDirect

Thin Solid Films

journal homepage: www.elsevier.com/locate/tsf

Ion beam analysis of a-C:H films on alloy steel substrate

T.F. Silva [a,*], M.V. Moro [a], G.F. Trindade [a], N. Added [a], M.H. Tabacniks [a], R.J. Santos [b], P.L. Santana [b], J.R.R. Bortoleto [b]

[a] Instituto de Física da Universidade de São Paulo, C.P. 66318, 05315-970 São Paulo, SP, Brazil
[b] Grupo de Plasma e Materiais, Universidade Estadual Paulista, 18087-180, Sorocaba, SP, Brazil

ARTICLE INFO

Article history:
Received 14 February 2013
Received in revised form 17 July 2013
Accepted 25 July 2013
Available online 1 August 2013

Keywords:
Amorphous hydrogenated carbon
Ion beam analysis
Plasma immersion ion implantation and deposition

ABSTRACT

An a-C:H thin film deposited by plasma immersion ion implantation and deposition on alloy steel (16MnCr5) was analyzed using a self-consistent ion beam analysis technique. In the self-consistent analysis, the results of each individual technique are combined in a unique model, increasing confidence and reducing simulation errors. Self-consistent analysis, then, is able to improve the regular ion beam analysis since several analyses commonly used to process ion beam data still rely on handling each spectrum independently. The sample was analyzed by particle-induced x-ray emission (for trace elements), elastic backscattering spectrometry (for carbon), forward recoil spectrometry (for hydrogen) and Rutherford backscattering spectrometry (for film morphology). The self-consistent analysis provided reliable chemical information about the film, despite its "heavy" substrate. As a result, we could determine precisely the H/C ratio, contaminant concentration and some morphological characteristics of the film, such as roughness and discontinuities.

1. Introduction

Thin films of hydrogenated amorphous carbon (a-C:H) can exist in two phases: diamond like carbon (DLC) and polymer like carbon, differing in the distribution of their carbon hybridization states (specifically, sp1, sp2 and sp3 bonds) and the atomic H content [1].

In the DLC phase, which is the most common application of a-C:H films, the hydrogen concentration may vary from less than 1% up to about 50% with significant amounts of sp3 type C bonds, giving it interesting physical and mechanical properties that are, to a certain extent, similar to those of diamond [2]. DLC films have the property of high tribological performance in a wide variety of operating environments, being established in many industrial applications due to their hardness [3], chemical inertness [4], optical transparency [5] and semiconductor properties [6]. A review on DLC, its properties and applications can be found in [7].

There is a need to characterize the elemental composition (H/C ratio and contaminants) of a-C:H films and, since they are usually thin (typically thinner than a micrometer), ion beam analysis (IBA) techniques are well suited for almost all the required elemental analyses [8].

IBA comprises a set of analytical techniques suited for material analysis, of which the most important are the following: particle-induced x-ray emission (PIXE) [9] used to determine the elemental concentration and trace elements ($Z > 11$) in the sample; elastic backscattering spectrometry (EBS) [10,11] used to quantify a unique element in the sample when a resonant non-Rutherford cross section is available; forward recoil spectrometry (FRS) [10,11] used when atoms from the sample recoiled by collisions of the beam are detected; and Rutherford backscattering spectrometry (RBS) [10,11], mainly used for concentration and depth profiling measurement, based on the detection of particles of the beam elastically backscattered to the detector. The concentration measured by RBS, in units of mass by unit of area, is related to the thickness of the film by its density.

Ion beam methods are commonly used for a-C:H characterization [1,8], but the combination of light elements, such as carbon and hydrogen, on a heavy element substrate, represents an analytical challenge for IBA techniques. A solution is the use of several techniques to provide complementary information about the sample, avoiding ambiguities related to limitations of each technique. However, the characterization of the film itself is usually derived from independent analysis of each measurement and the simple use of different techniques may lead to mistakes if the analysis is not done self-consistently.

In this paper, we present a self-consistent IBA analysis of an a-C:H film deposited by plasma immersion ion implantation and deposition (PIIID) on 16MnCr5 alloy steel. The self-consistent approach adopted in this study combines several ion beam measurements in a unique model where experimental data of all measurements are fitted simultaneously. The simultaneous fit of all the spectra means that information obtained from each technique is used as a boundary condition wherever applicable on the others. In this way, all information about the sample emerges consistently from the set of spectra analyzed, providing a powerful tool to model the sample unequivocally and reliably [10], and even to characterize some morphological aspects of the film, like roughness

* Corresponding author.
E-mail address: tfsilva@if.usp.br (T.F. Silva).

0040-6090/$ – see front matter © 2013 Elsevier B.V. All rights reserved.
http://dx.doi.org/10.1016/j.tsf.2013.07.073

(measure of non-uniformities) and the presence of discontinuities. We also present a study of the main parameters that influence the measurement uncertainty for this approach.

2. Methods

We used four IBA techniques to characterize an a-C:H film deposited by PIIID on a 16MnCr5 alloy steel substrate. The selection of techniques was done in order that they should complement each other, resulting in a complete characterization of the sample's composition. High sensitivity makes PIXE well suited to determine trace elements of the sample but with no depth profile information; RBS analysis has poorer elemental discrimination but very good accuracy for depth profiling and stoichiometric determination; EBS analysis is appropriate to enhance the carbon signal for quantification in low concentrations and high background counts due to the heavy element substrate; FRS analysis was used for hydrogen measurement, completing the analytical set.

The measurements were performed in pairs using two different experimental setups. In the first one, a surface barrier detector was positioned at 170° and an x-ray detector at 90°, both with respect to the direction of the incident beam (see schematic in Fig. 1a). With this setup, PIXE analysis can be done together with ion scattering analysis (such as EBS, FRS or RBS). EBS analysis was done with a 1.73-MeV proton beam to make use of a (p,C) resonance at this energy, and the spectra were fitted using SIMNRA [12,13] code and cross-section data of reference [15].

In the second setup, two surface barrier detectors were used: the first at 170° and the other at 30°, both with respect to the direction of the incident beam (see schematic in Fig. 1b). In the detector located at 30°, a 11-μm-thick aluminum foil was used as stopper filter to assure that only hydrogen recoiling from the sample reached the detector. The accuracy of the FRS measurements and the thickness of the stopper filter were checked with the analysis of standard polymers samples with different H/C ratios. The 80° beam incidence angle on the sample

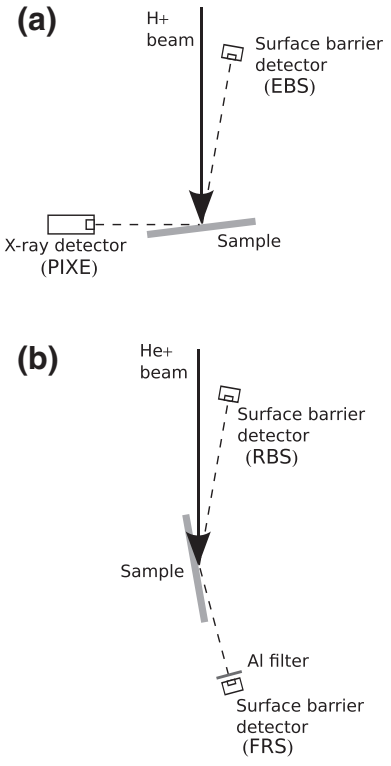

Fig. 1. Schematic of the experimental setup. (a) for PIXE and EBS, (b) for FRS and grazing angle RBS.

was chosen in order to enable the FRS measurement, and also to provide a grazing angle of incidence for the RBS analysis, increasing its sensitivity to very thin films. The choice of a 2.2-MeV He + beam was made as a standard value for RBS analysis in our facility and determined the choice of the aluminum filter thickness. When the beam strikes the sample, some of the beam particles will be backscattered to the detector located at 170°, and some of the hydrogen at the surface of the sample will be scattered towards the detector located at 30°. These measurements correspond to RBS and to FRS, respectively. The RBS and FRS spectra were fitted using the SIMNRA [12,13] code. At this beam energy, the cross section for a H recoiled by He beam deviates from the Rutherford cross section [16], and can be found in reference [17].

Using the PIXE analysis, we can determine the presence of contamination in the film. The EBS analysis determines the concentration of carbon in the film, which, combined with the hydrogen determination by FRS analysis, can give the H/C ratio. The RBS analysis in a grazing angle enables the analysis of some morphological aspects of the film.

Finally, the self-consistent analysis consisted in the interactive simulation, with the SIMNRA [12,13] code, of the EBS, FRS and the RBS spectra. The simulated model for the sample that best fitted all the spectra simultaneously was considered the correct model for the sample.

2.1. Sample preparation

The alloy steel substrate was prepared as a slice with 20 × 20 × 5 mm^3, and sequentially sanded with 120, 200, 600 and 1200 grains per square centimeter sandpapers. After sanding, the sample was polished with felt paper and alumina powder with grain sizes in the 3- to 6-μm range and washed with deionized water followed by isopropyl alcohol. Finally, the sample was submitted to a plasma technique for oxide removal of the surface.

The thin film deposition was performed by PIIID [7] with no exposure to air. The plasma was generated in a 4:1 mixture of methane gas (CH4) and Ar; the radio frequency and power to generate the plasma were 13.56 MHz and 100 W, respectively. The deposition process lasted for 1800 s. During this period, the sample was polarized with high-voltage pulses of −3.6 kV for 30 μs and 300 Hz frequency. Pulsing the high-voltage produces acceleration of the positive ions of the plasma in the direction of the sample. These ions are implanted in the surface of the substrate forming a very thin interface layer that improves adhesion of the film on the substrate. It is a standard process of PIIID. The thickness of the film was measured as 61(14) nm by profilometry (Instrumentation: Veeco, model Dektak 150).

2.2. Experimental details

The beam energy calibration was made using $^{16}O(\alpha,\alpha)^{16}O$ resonances at 3.031(1) MeV [14] and the $^{12}C(p,p)^{12}C$ resonance at 1.734(5) MeV [15]. Besides, a sample of ultra-dense amorphous carbon was used to check the terminal voltage at the $^{12}C(p,p)^{12}C$ resonance prior to the EBS measurements.

The accuracy of the detector angular positioning is better than 0.5°. The solid angle was determined analyzing the backscattering of 2.2 MeV α-particles on an amorphous silicon sample due to the Rutherford character of its cross section and its well-known stopping power, which presents good agreement between experiment and the calculation [10]. The energy resolution (full width at half maximum) is 25 keV for the surface barrier detectors and 144 eV for the x-ray detector, at Mn-Kα using ^{55}Fe.

The charge collection system provides accuracy better than 1%, confirmed by a calibrated current source and by RBS analysis on an amorphous silicon sample (the sample holder is surrounded by a suppressor in a negative high-voltage potential to avoid losses by emission of secondary electrons).

3. Results and discussion

3.1. PIXE measurements

The PIXE analysis was made by comparison between the spectra of two samples: a blank (without a-C:H thin film), and one with the a-C:H layer. It is possible to observe in Fig. 2 that both spectra are very similar and a small Ar contamination in the covered sample can be observed. Signals from Fe, Cr and Mn are due to elements present in the substrate.

A sample of Kapton, with 21 keV-Ar implanted in a concentration of $3.6(8) \times 10^{15}$ at/cm^2, was used as standard to measure the concentration of Ar in the a-C:H film. SRIM [18] calculation showed average depth of Ar as 35 nm in kapton, giving a negligible correction factor due to x-ray attenuation for the K-a line of Ar (0.9993 correction factor coefficient) calculated with XCOM [19].

The Ar concentration obtained was $2.8(8) \times 10^{15}$ at/cm^2. This value is close to the detection limit of PIXE technique under these circumstances and could not be detected by the scattering analysis since this concentration is under their detection limit. So that, the Ar contamination was not considered in the model for the fitting of EBS, FRS and RBS techniques.

3.2. EBS measurements

The EBS analysis showed a very thin film of C on top of the 16MnCr5 steel substrate (see Fig. 3). The film is too thin to enable a profile measurement since the width of the C peak is dominated by the detector resolution. Thus, just the quantification of the C content was possible.

3.3. FRS measurements

The FRS analysis showed a hydrogen peak (see Fig. 4), which is not completely dominated by the detector resolution but the information on the depth profile is not accurate due to geometrical factors and straggling in the stopper filter. However, as in the EBS case, the height of the peak enables the quantification of the H content.

The presence of a small contamination of H on the surface of the blank sample was observed (dashed line in Fig. 4). This contamination is probably due to formation, after the plasma cleaning process, of a thin layer of hydrogen-containing molecules, originating additional hydrogen yield from the surface. These counts do not exceed 6% of the counts for the film deposited sample.

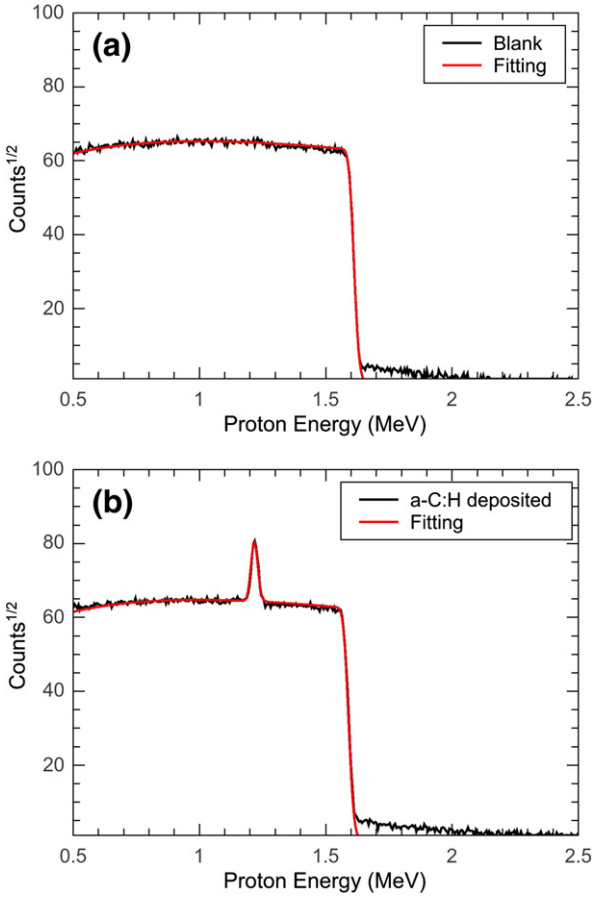

Fig. 3. EBS analysis for carbon quantification. (a) The blank sample spectrum containing just alloy steel; (b) the C peak for quantification.

3.4. RBS measurements

This measurement completes the set of techniques used in the analysis. Fig. 5 shows a comparison between RBS spectra for the blank sample and for the a-C:H deposited sample. It is possible to observe the formation of a step-like profile in the spectrum of the deposited sample (see Fig. 5b) where the first trailing edge extends up to 1.67 MeV, which is the same energy as the trailing edge in the spectrum of the blank sample (see Fig. 5a). This profile implies the presence of substrate atoms on the surface of the sample. However, this information by

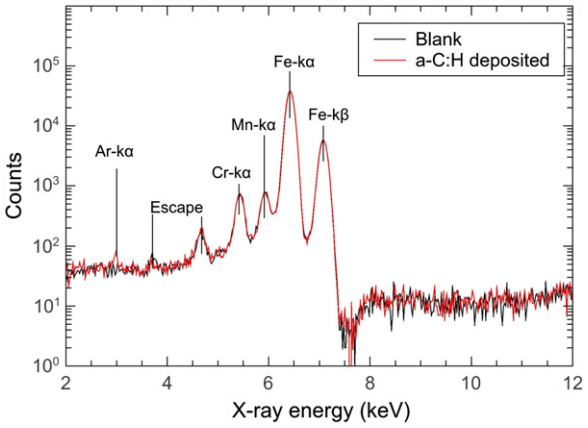

Fig. 2. X-ray spectra for PIXE analysis. Detail of the x-rays lines of elements Mn, Cr, Fe (in both samples) from the alloy steel, and the Ar contamination (on the sample with a-C:H film), due to deposition technique.

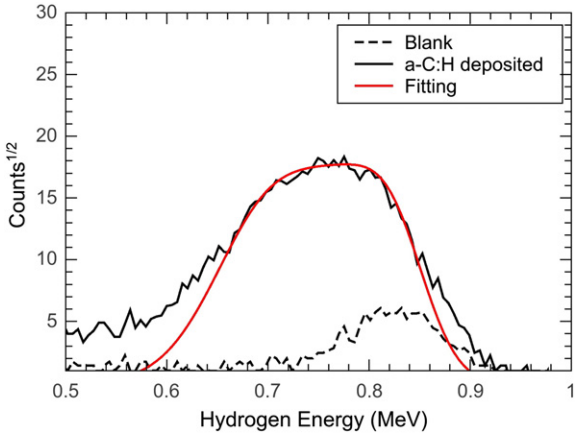

Fig. 4. FRS analysis for hydrogen quantification. The spectrum of the sample with the a-C:H film is compared with the blank sample that presents a small concentration of H on the surface.

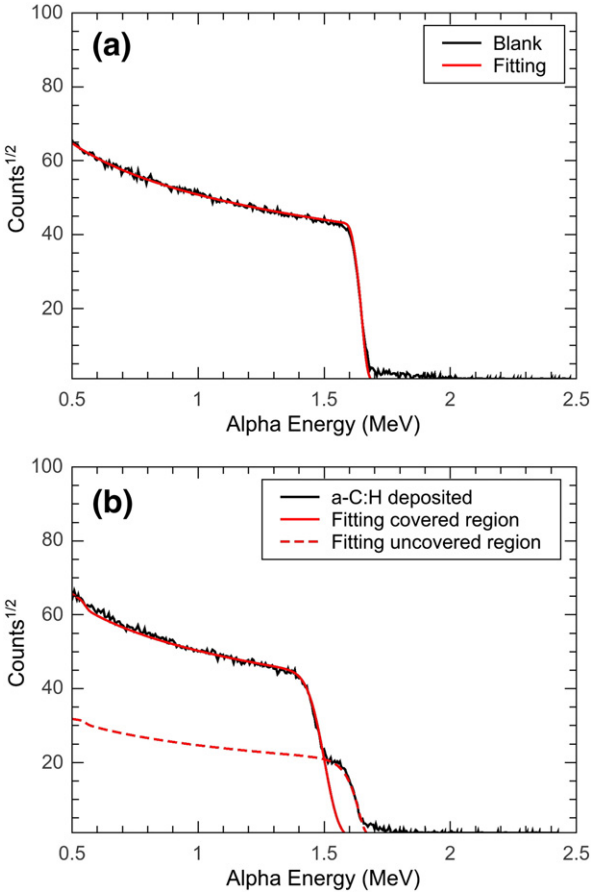

Fig. 5. RBS analysis for morphological examination of the a-C:H film. (a) The blank sample spectrum; (b) the sample with a-C:H film.

itself is ambiguous and cannot tell us if these atoms are contained in the film as a contamination or if they are due to exposure of the substrate.

For this reason, we used optical microscopy imaging to examine the surface of the sample. The presence of regions with the substrate exposed was confirmed by the microscopy image presented in Fig. 6, which was used to measure the uncovered area as 20% of the covered area (not continuous). As a consequence, the spectrum in Fig. 5b must be treated as a combination of two spectra: of a blank sample (uncovered area) and a sample with film (covered area), both weighted by the fraction of the incident charge on each region, determined from the ratio uncovered/covered areas measured using the microscopic image (assuming a homogeneous beam).

3.5. Self-consistent analysis

Attempts to fit all the spectra simultaneously using a model with heavy-elements contaminants in the film were frustrated. However, using the ratio uncovered/covered areas measured in the microscopy image to correct the fit for substrate exposure, we were able to find a model that fitted all the spectra simultaneously with no heavy-element contamination in the film. This configuration proved to be the model that was able to fit all experimental data. The Ar contamination (measured by PIXE) was not considered in the sample for the fitting of EBS, FRS and RBS data since it is under the detection limit for these techniques. The corresponding fits for each technique are presented in Figs. 3, 4 and 5.

The self-consistent analysis played an important role in solving the RBS ambiguity: if heavy-element contamination was present in the film, its stopping power would be different and the EBS, FRS and RBS data would not be simultaneously fitted. Finally, with all

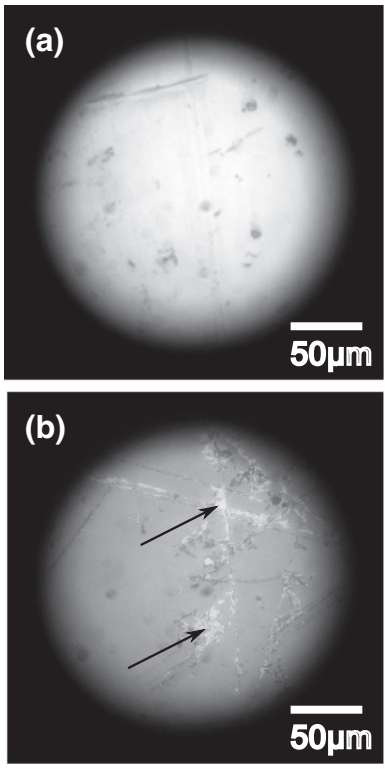

Fig. 6. Optical image with 63× amplification. (a) Sample with no deposition; (b) deposited sample. The arrows indicate two examples of discontinuities of the film.

this information, we can say that, within our detection limits and uncertainties, there is no evidence of heavy-element contamination in the film.

The quantities of carbon and hydrogen in the film were determined as $840(60) \times 10^{15}$ at/cm^2 and $148(17) \times 10^{15}$ at/cm^2, respectively. The H/C ratio was determined as 0.17(2), with a 12% uncertainty. Fitting the inclination of the second trailing edge of the RBS analysis allowed the estimation of the normalized standard deviation of the areal density (roughness) of the film as 50%. This is a measure of non-uniformities of the film and is highly affected by the presence of film discontinuities. The high value of the roughness can be explained by combination of a high roughness of the substrate and the thin thickness of the film together with the existence of film discontinuities.

The total measurement uncertainty of the self-consistent analysis was calculated taking into consideration the parameters that most influence the final result [10]. A summary of this evaluation is presented in Table 1.

4. Conclusions

In this paper, we explored the use of self-consistency of IBA techniques in the analysis of an a-C:H thin film deposited by PIIID method.

Table 1
Summary of results and experimental parameters that most influence the total uncertainty. The total uncertainty was calculated using standard propagation formulas.

	C	H
Quantity ($\times 10^{15}$ at/cm^2)	840 (60)	148 (17)
Fitting	1.9%	3.8%
Energy	4.7%	7.1%
Cross section	5.0%	6.0%
Stopping power	0.3%	4.8%
Filter	–	2.9%
Total	7.1%	11.5%

With the PIXE measurement, a small quantity of argon was found as a contaminant. Using the EBS analysis, it was possible to enhance the signal from carbon and determine its absolute concentration with 7.1% accuracy, despite the heavier element substrate. With the FRS analysis, we determined the absolute hydrogen concentration with 11.5% accuracy. The H/C ratio was determined with 12% accuracy. Finally, the RBS data obtained in a grazing angle enabled the analysis of some morphological aspects of the film: not only was it possible to estimate the roughness of the film but also its discontinuities, the last confirmed by optical microscopy.

Using the background counts we estimated the lower detection limit as 100 at. ppm for carbon and 200 at. ppm for hydrogen, for the combination a-C:H film over alloy steel substrate.

The combination of several IBA techniques in a self-consistent analysis proved to be useful to improve and to extend the information that could be obtained from independent measurements.

Acknowledgements

The authors acknowledge financial support from Brazilian funding agencies: CNPq, CAPES and Fapesp.

The authors also acknowledge the Laboratory of Ion Beam Analysis of the University of São Paulo (LAMFI-USP) for the IBA measurements, M.Sc. C. L. S. Risi for the optical microscopy images, Dr. C. L. Rodrigues for the Ar implantation and Dr. M. N. Martins for suggestions on the manuscript.

References

[1] D. Gracin, M. Jaksica, I. Bogdanovic-Radovica, Z. Medunica, T. Cara, B. Pracekb, Vacuum 67 (2002) 519.
[2] A. Grill, Diam. Relat. Mater. 8 (1999) 428.
[3] W. Dai, P.L. Ke, M.W. Moon, Thin Solid Films 520 (2012) 6057.
[4] R. Compton, J. Foord, F. Marken, Electroanalysis 15 (2003) 1349.
[5] Š. Meškinis, V. Kopustinskas, A. Tamulevičienė, S. Tamulevičius, G. Niaura, J. Jankauskas, R. Gudaitis, Vacuum 84 (2010) 1133.
[6] V.V. Buniatyan, V.M. Aroutiounian, J. Phys. D 40 (2007) 6355.
[7] J. Robertson, Mater. Sci. Eng. Rep. 37 (2002) 129.
[8] J.-P. Hirvonen, J. Koskinen, P. Torri, R. Lappalainen, A. Anttila, Nucl. Instrum. Methods B 118 (1996) 596.
[9] S.A.E. Johansson, J.L. Campbell, K.G. Malmqvist, Particle-Induced X-Ray Emission Spectrometry (PIXE), John Willey & Sons, New York, 1995.
[10] C. Jeynes, N.P. Barradas, E. Szil'agyi, Anal. Chem. 84 (2012) 6061.
[11] W.-K. Chu, J.W. Mayer, M.-A. Nicolet, Backscattering Spectrometry, Academic Press, New York, 1978.
[12] M. Mayer, Tech. Rep. IPP 9/113, Max-Placnk-Institut fur Plasmaphysik, Garching, 1997.
[13] M. Mayer, in: J.L. Duggan, I.L. Morgan (Eds.), Proceedings of the 15th International Conference on the Application of Accelerators in Research and Industry, American Institute of Physics Conference Proceedings, 475, 1999, p. 541.
[14] J. Demarche, G. Terwagne, J. Appl. Phys. 100 (2006) 124909.
[15] S. Mazzoni, M. Chiari, L. Giuntini, P.A. Mandò, N. Taccetti, Nucl. Instrum. Methods B 136–138 (1998) 86.
[16] J.E.E. Baglin, A.J. Kellock, M.A. Crockett, A.H. Shih, Nucl. Instrum. Methods B 469–474 (1992) 64.
[17] C.S. Kim, S.K. Kim, H.D. Choi, Nucl. Instrum. Methods B 229-237 (1999) 155.
[18] J.F. Ziegler, M.D. Ziegler, J.P. Biersack, Nucl. Instrum. Methods B 1818–1823 (2010) 268.
[19] M.J. Berger, J.H. Hubbell, S.M. Seltzer, J. Chang, J.S. Coursey, R. Sukumar, D.S. Zucker, XCOM: Photon Cross Section Database (version 1.2), National Institute of Standards and Technology, Gaithersburg, MD, 2005. (available URL: http://physics.nist.gov/xcom).